

Truncated lognormal distributions and scaling in the size of naturally defined population clusters

Álvaro Corral,^{1,2,3,4} Frederic Udina,⁵ and Elsa Arcaute⁶

¹*Centre de Recerca Matemàtica, Edifici C,
Campus Bellaterra, E-08193 Barcelona, Spain*

²*Departament de Matemàtiques, Facultat de Ciències,
Universitat Autònoma de Barcelona, E-08193 Barcelona, Spain*

³*Barcelona Graduate School of Mathematics, Edifici C,
Campus Bellaterra, E-08193 Barcelona, Spain*

⁴*Complexity Science Hub Vienna, Josefstädter Straße 39, 1080 Vienna, Austria*

⁵*Department of Economics and Business, Universitat Pompeu Fabra,
Ramon Trias Fargas 25-27, E-08005, Barcelona, Spain*

⁶*Centre for Advanced Spatial Analysis, University College London,
90 Tottenham Court Road, London, W1T 4TJ, UK*

Abstract

Using population data of high spatial resolution for a region in the south of Europe, we define cities by aggregating individuals to form connected clusters. The resulting cluster-population distributions show a smooth decreasing behavior covering six orders of magnitude. We perform a detailed study of the distributions, using state-of-the-art statistical tools. By means of scaling analysis we rule out the existence of a power-law regime in the low-population range. The logarithmic-coefficient-of-variation test allows us to establish that the power-law tail for high population, characteristic of Zipf's law, has a rather limited range of applicability. Instead, lognormal fits describe the population distributions in a range covering from a few dozen individuals to more than one million (which corresponds to the population of the largest cluster).

PACS numbers:

INTRODUCTION

Cities are expected to experience enormous growth in the next decades, but already nowadays, they can be considered in some sense as the largest structures built by humankind. However, in contrast to other human constructions, cities develop from social and economic processes combined with top-down planning. Social and economic processes in their turn depend on technological and scientific advances. So, cities are complex systems driven by self-organization, where its fundamental constituents (the individuals) participate in a vast number of different types of interactions that keep the city alive [1]. In fact, the analogy between cities and living organisms is not just a metaphor but a very deep insight [2].

Probably, the first characterization of any entity is in terms of its size, and this also holds for complex entities. It is well known that for cities, their size (measured for instance in number of inhabitants) is broadly distributed (there are cities of vastly different sizes, taking a broad definition of a city as a “human settlement”). Then, a statistical description is necessary. Several statistical models for city size have been proposed, with the most important one being Zipf’s law [3], which states that, given a country or a large region, the probability mass function $f(s)$ of city size s is given by a power-law (pl) distribution,

$$f_{pl}(s) \propto \frac{1}{s^\beta},$$

with the symbol “ \propto ” denoting proportionality and the exponent β taking values close to two (an important requirement is that the exponent has to be larger than one). The law should apply at least to the largest cities, i.e., for the upper tail of the size distribution, and so one has in mind cities and towns but not necessarily small villages. It is a remarkable fact that Zipf’s law seems to hold in many other systems in which individuals gather into some sort of groups or classes (companies [4], religions [5]), and where the “individuals” can be anything from animals [6] to links in the Internet [7], word tokens in a text [8], or combinations of musical notes [9].

Nevertheless, there have been authors who have argued in favor of other models; in particular, for city-size distribution the lognormal model has been proposed as the most remarkable alternative to Zipf’s law, and some debate has arisen [10–12]. This debate can be put in the broader context of the adequacy of power-law fitting procedures [5, 13–18], but is certainly different from the controversy about power-law relations in “urban metabolism” or urban allometry [2, 19, 20]. Nevertheless, at the core of both problems is the proper use

of statistical tools, which is part responsible of the recent, unfortunate, and deep problem known as reproducibility crisis, or replicability crisis [21, 22].

In any case, one can realize that there is a degree of arbitrariness in city-statistics research, related to the definition of what a city is. If the usual administrative delimitations (which were established, in general, following criteria developed many decades or centuries ago) are used for today urban agglomerations, to which extend are the results for city-size distributions not just an artefact of old bureaucracy? Clearly, more realistic and scientific definitions of the concept of city are necessary. This has been attempted by several authors [23–25], who have introduced the concept of naturally-defined cities, see in particular the citations in Refs. [19, 23, 26].

In the present paper we use population data of high resolution to construct clusters of population, which we identify with cities, whose size distribution is scrutinized with state-of-the-art statistical tools. In the next section we describe the data; in Sec. 3 we explain the several similar procedures used to construct the population clusters (our definition of cities); and in Sec. 4 we present our statistical study of the size of clusters, using scaling analysis, the logarithmic-coefficient-of-variation test, as well as truncated-lognormal and power-law fits of the resulting distributions. We anticipate that the lognormal distribution is much more suitable than the power law to describe the cities arising from the analyzed dataset and the city-definition introduced. Also, the importance of spatial correlations in the number of inhabitants to get a broad cluster-size distribution is clearly established.

DATA

Here we approach the problem of city definition and the validity of Zipf’s law using high-resolution data for the scatter of a population through a territory. The territory under study is Catalonia (*Catalunya*), located in NE Spain and whose capital is the colorful city of Barcelona. Catalonia has a population of about 7,500,000 inhabitants in a area of 32,000 km², which yields an average density around 230 inhabitants per km² and classifies Catalonia as a highly populated area. Note that these figures are similar to those of some small European countries, such as Switzerland for example.

In Spain, the municipality councils (*ayuntamientos*) collect a population register called *Padrón Municipal de Habitantes*. All citizens are required to be registered in some mu-

nicipality and actually it is necessary to be registered to access most of the administrative services like health, education, etc. The coordination of the registers of all municipalities in the country is done by the Spanish *Instituto Nacional de Estadística* (<http://www.ine.es>), which sends the information referred to Catalonia to the Catalan *Institut d'Estadística de Catalunya* (IDESCAT, <http://www.idescat.cat>). The processing of the registers is an important step because it guarantees their high quality: duplicated entries are removed as are people deceased or registered in a foreign-country embassy.

In the last years, IDESCAT has undertaken the task of georeferencing each individual's postal address present in the register, by means of the geocoding web service of the *Institut Cartogràfic i Geològic de Catalunya* (<http://www.icgc.cat>), which assigns geographical coordinates to each postal address. The complete procedure including the imputation for missing data is detailed in Ref. [27].

The data that we have used for our study is the georeferenced population of Catalonia at January 1, 2013, with a total population of $M = 7,586,888$ inhabitants in 989,997 places of residence (i.e., domicile buildings), and with a 7.6 % of errors in the georeferencing for which the procedure of imputation is applied [27]. This register can be considered as high resolution population data, even of higher resolution than the data used in Refs. [28, 29] (which was 100 and 200 m, respectively; our is about few meters, corresponding to the minimum distance between places of residence). The spatial distribution of the complete data set is displayed in Fig. 1.

CLUSTERS OF POPULATION

Grid approach

In order to construct our aggregations of population, we first work using a simple (equirectangular) projection of longitude and latitude into Cartesian coordinates, which introduces very little distortion due to the small extent of the territory. We cover the resulting projection by a grid composed by identical square cells, each of fixed width ℓ in degrees and projected area $\ell \times \ell$, aligned with the longitude-latitude axes. In a second, more refined approach, we transform longitude and latitude into distances (using that 1° in latitude is equal to 111.1 km and 1° in longitude is about 83 km at latitude 41°), and introduce again a

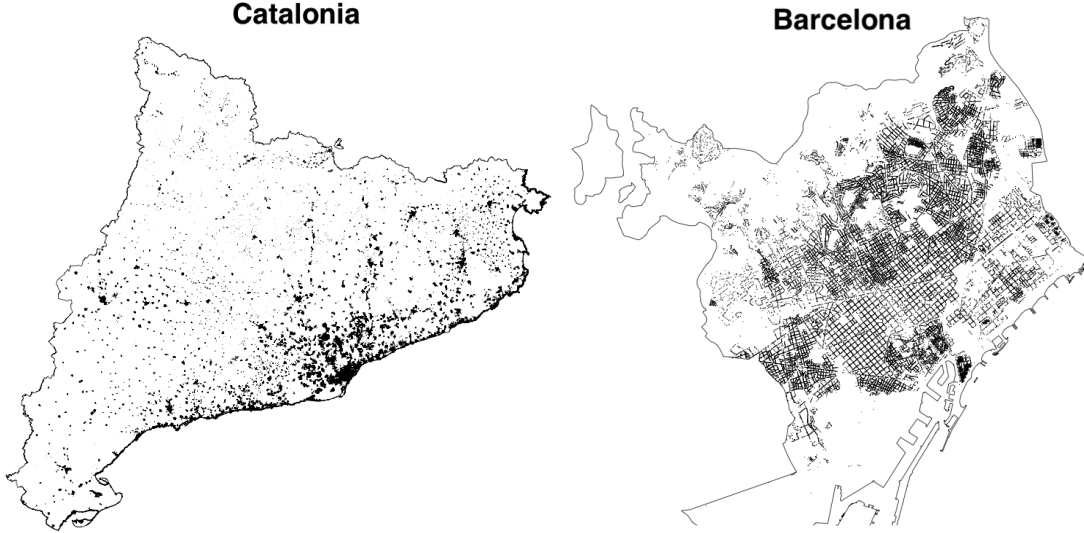


FIG. 1: (a) Whole dataset: Latitude and longitude of the 7,586,888 inhabitants of Catalonia at January 1, 2013. (b) Zoom of the data around the Barcelona zone. Notice that we are representing the coordinates of the residence place of each individual, so, the high resolution of the data becomes apparent in this plot.

square grid. We call these two approaches grid-in-degrees and grid-in-km, respectively. We advance that both of them will lead to essentially the same results.

Note that a square in longitude-latitude is equivalent to a rectangle in distance, and vice versa, so, in terms of distances our two types of grids are rectangles (with fixed aspect ratio) and squares, respectively. When we report the width ℓ of a cell in degrees it is implicit that we are dealing with the first approach, and when ℓ is in meters or in km we will follow the second one.

The next step is counting the number of inhabitants h in each cell. For reasonable values of the cell width (for instance, $\ell = 0.001^\circ$) the resulting h turns out to be broadly distributed, from one inhabitant per cell to many thousands (we will disregard unpopulated cells, for reasons that will become clear later). For the sake of illustration, we display the corresponding probability mass function $f(h)$ in Fig. 2(a) for different values of the cell width ℓ for the grid-in-km approach, confirming the broadness of the distribution (dependence of $f(h)$ on ℓ is obviated in the notation). The population density in each cell can be calculated straightforwardly as $\rho = h/\ell^2$, and its probability density $f(\rho)$ (the probability density of the population density) is shown in Fig. 2(b), in units of km^2 . It is obvious that, for the

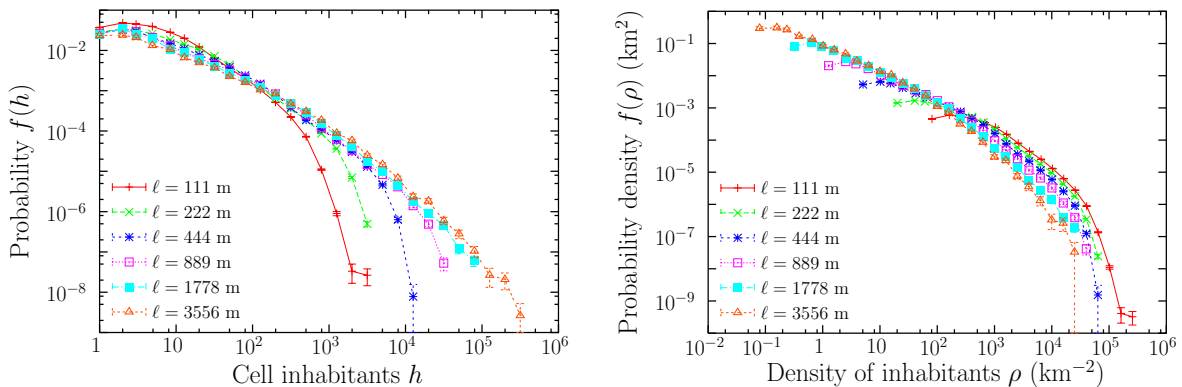


FIG. 2: (a) Empirical probability mass functions $f(h)$ of number of inhabitants h per cell, for several values of cell width ℓ , in the grid approach, using the grid-in-km procedure. (b) Corresponding empirical probability densities of population density per cell. Observe the enormous variability, from less than 0.1 inhabitant per km^2 to more than 10^5 . Unpopulated cells are not considered.

same ℓ , both distributions, $f(h)$ and $f(\rho)$, have the same shape, with the only difference of the scale factor ℓ^2 . The fact that we consider $f(h)$ as a probability mass function and $f(\rho)$ as a probability density is not relevant, and comes from the consideration of h as a discrete variable and ρ as a continuous one, but this difference does not carry any deep meaning.

Under the present grid approach, our definition of city is based on the aggregation of adjacent occupied cells. This is a natural definition, previously used in Ref. [23]. We will consider a cell as occupied if its population is greater or equal than a threshold value, and unoccupied otherwise. Naturally, the most immediate value for the population threshold is one [23], but other prescriptions are possible; the advantage of our high-resolution data is that the threshold can be made as small as desired, in contrast for instance to Ref. [19]. For this reason, the occupation threshold is equal to one in this work.

More concretely, as in the problem of site percolation [30, 31], a set of nearest-neighbor occupied cells surrounded by non-occupied nearest neighbors defines a (connected) cluster [23]. These clusters will constitute a proxy for cities (we identify the clusters by means of a variation of the classic Hoshen-Kopelman algorithm); and we may generically refer to *clusters of population*. As in this framework the definition of what a cluster (or a city) is depends on ℓ , and there is no a-priori way to find an optimum ℓ , different values of this

parameter will be considered, in order to test the robustness of the results.

The size s of a cluster is defined as its total population (do not get confused with its total area), i.e., for a cluster i ,

$$s_i = \sum_{\forall j \in i} h_j, \quad (1)$$

where the sum runs for all cells j that are part of cluster i (obviously, the cluster definition implies that no cell can belong to more than one cluster). Note that the cluster sizes can range from 1 to the whole population of the territory (depending on the spatial location and on the selected value of the underlying cell width ℓ). Then, one should not find strange in this context to talk about cities with just one inhabitant, although it is more proper to refer to them as size-one clusters. Table I provides, for different values of ℓ , the total number of clusters and the size of the largest one (in terms of numbers of inhabitants) resulting from applying our procedure. As an example, Fig. 3 shows the largest cluster for cell width $\ell = 0.002^\circ$.

Ball approach

An alternative approach to define clusters of population can be done using the CCA (City Clustering Algorithm [23]); this percolation method has been previously employed by one of the authors, see Ref. [26]. Its implementation can be done using a DBSCAN algorithm (Density-based spatial clustering of applications with noise [32]), changing the distance at each iteration. The approach is based on considering “balls” of a fixed radius ℓ , centered on each individual; given a radius value ℓ , a cluster is defined as the set of all balls that overlap with (or touch) at least another ball in the cluster. This means that any individual in the cluster is at a distance smaller than (or equal to) 2ℓ of at least another individual in the cluster. The distance is measured in meters over the Earth surface.

The cluster population is obtained again as the sum of individuals contained in the cluster. One could still use Eq. (1), but then h_i has to be interpreted as the number of individuals in the center of each ball and the sum has to run for all balls j associated to cluster i . We refer to this procedure as the ball approach, and it has clear advantages with respect the grid approach that it is not affected by the arbitrariness of setting an origin of coordinates for the grid and that it avoids problems in defining a grid over a sphere (mainly if one pretends to extend this kind of analysis to much larger regions). The properties of the clusters resulting

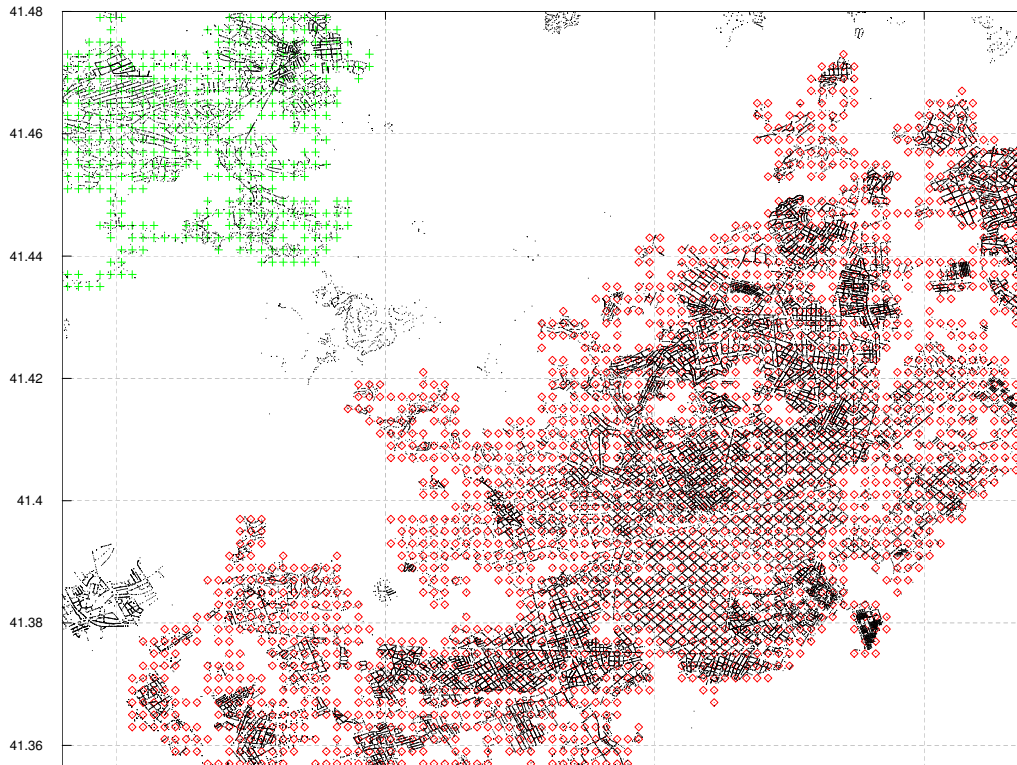


FIG. 3: Cluster associated to Barcelona urban area (in red), for cell width $\ell = 0.002^\circ$. The cluster, which is the largest one for this ℓ , includes part of other municipalities in addition to Barcelona, but there are parts of the Barcelona municipality not included in the cluster. Part of the second-largest cluster (in green) is also shown.

from this approach are included in Table I. Once the population has been computed for each cluster, the cluster-size distribution follows immediately; this will be shown in the next section.

ANALYSIS AND RESULTS

In order to investigate the validity of Zipf's law for the clusters of population, we consider, as in Ref. [5], the point of view of the distribution of sizes (in contrast to using the rank-size relation, which can lead to confusing interpretations [33]). The advantages of this choice are discussed in Ref. [34], see also Ref. [8]. Figure 4 displays the corresponding cluster-size distributions in terms of the empirical probability mass function $f(s)$, for different values of ℓ (the notation obviates the dependence on ℓ) and for the three approaches (grid-in-degrees,

grid-in-km, and balls).

We clearly observe the broadness of the distributions, ranging from population one to more than one million (more than 6 orders of magnitude). The smoothness of the distributions is also apparent, with no change of behavior for all the range, except, perhaps, in the transition from one inhabitant to two, where the probability of former value (one) is decreased with respect to the latter (in a sense, one could speculate that a fundamental unit of human population could be the couple, instead of the single individual). In contrast, the usual distribution of population for the municipalities (also included in the plot) shows a clear transition around population 200; thus, the presence of villages with population below this value is greatly diminished. With our definition of population clusters, instead, the broadness and smoothness of the distributions do not allow to find discontinuity points to distinguish between cities and towns, and between towns and villages (except for the change of behavior between clusters of size one and two, as just mentioned). In addition, the proximity of the distributions to a straight line in log-log representation suggests a power-law behavior. However, it is misleading to use visual information of linear behavior in log-log plots as an indication of power-law behavior [5, 13]. Rigorous statistical tools are required [5, 15, 17, 18].

Scaling analysis

As a first step before moving to more quantitative methods, we apply scaling analysis to the distributions (do not get confused between scaling and power-law behavior; the distinction will become clear in what follows). When one has several broad distributions, which depend on some parameter (ℓ in our case), scaling analysis can be a very informative tool [35]. Let us assume that, for different values of the cell width ℓ , the cluster-size distributions $f(s)$ scale with some scale parameter θ (which depends on ℓ) as

$$f(s) \simeq \frac{K}{\theta} G\left(\frac{s}{\theta}\right),$$

where K is a normalization “constant” (which could depend on θ) and G is the scaling function (which is the same no matter the value of θ , i.e., of ℓ). It turns out that when, for small arguments, G does not behave as a power law, or behaves as power law with exponent

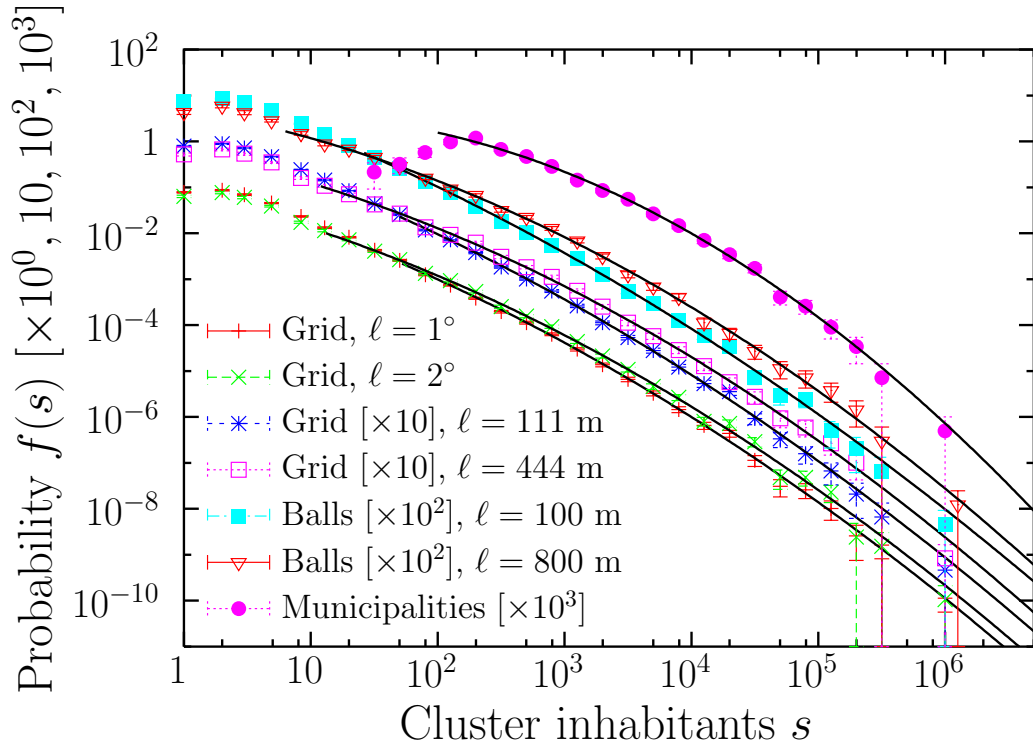


FIG. 4: Empirical probability mass functions $f(s)$ of cluster size s (in number of inhabitants) for several values of cell width ℓ , using: square grid in longitude-latitude (grid-in-degrees, bottom curves), square grid in distance (grid-in-km, y -axis multiplied by a factor 10, for clarity sake), and ball approach (y -axis multiplied by a factor 100). Results for the usual approach based on municipalities are also included, for the sake of comparison. Continuous lines are lognormal fits.

smaller than 1, the scaling law can be rewritten as

$$f(s) \propto \frac{1}{\langle s \rangle} G\left(\frac{s}{\langle s \rangle}\right),$$

due to the fact that the mean $\langle s \rangle$ scales linearly with θ and the constant K is a true constant (K and the constant relating $\langle s \rangle$ to θ are absorbed into G).

However, when for small arguments, G diverges as a power law with exponent α greater than one (but smaller than two), the previous scaling law is not valid and one instead has

$$f(s) \propto \frac{1}{\theta} \left(\frac{m}{\theta}\right)^{\alpha-1} G\left(\frac{s}{\theta}\right) \propto \frac{\langle s \rangle^3}{\langle s^2 \rangle^2} G\left(\frac{\langle s \rangle s}{\langle s^2 \rangle}\right), \quad (2)$$

as $\langle s \rangle \propto \theta^{2-\alpha}$ and $\langle s^2 \rangle \propto \theta^{3-\alpha}$, with m the minimum value of s (below which $f(s)$ is zero) and $\langle s^2 \rangle$ the second moment of the distribution (see Ref. [35]). In fact, this new scaling law

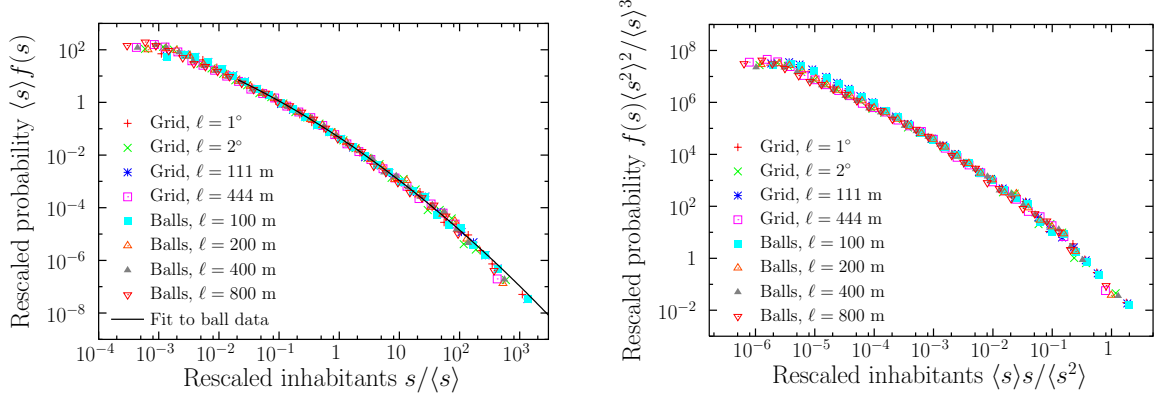


FIG. 5: (a) Empirical probability mass functions $f(s)$ rescaled by their mean value, $\langle s \rangle$ for some values of ℓ in the grid-in-degrees, grid-in-km, and ball approaches. The curve is the fit corresponding to the ball approach, as shown in the table. (b) Same probability mass functions using the non-trivial rescaling given by Eq. (2), see also Ref. [35]. The scalings in (a) and (b) can be considered as visually equivalent, which rules out the existence of a power-law with $\alpha > 1$ for small s . This could be made more quantitative using the collapse algorithm of Ref. [36].

is also valid in the other case ($\alpha < 1$ or absence of power law), due to the trivial scaling $\langle s \rangle \propto \theta$ and $\langle s^2 \rangle \propto \theta^2$ there, but the reciprocal is not true. Note that now we refer to the power-law exponent as α , in order to distinguish it from β , the power-law exponent at the large- s tail.

Therefore, estimating the moments from the sample and plotting, for different values of the cell width, $\langle s \rangle f(s)$ versus $s/\langle s \rangle$ as well as $\langle s^2 \rangle^2 f(s)/\langle s \rangle^3$ versus $\langle s \rangle s / \langle s^2 \rangle$, one will be able to check not only if a scaling law holds, but if for small arguments the distribution has a power-law shape with exponent in the range $1 < \alpha < 2$. This is done in Fig. 5 for the three representations (grid-in-degrees, grid-in-km, and balls); the data collapse for all analyzed ℓ indicates that both scaling laws are indeed fulfilled, and this implies that the power-law behavior (with $\alpha > 1$) can be discarded. The data collapse also shows that for different cell width ℓ , all analyzed cluster-size distributions have (roughly) the same shape, but at different characteristic scale, and this shape is not a power law (with $\alpha > 1$), at least for small s .

Residual logarithmic coefficient of variation

Still it could happen that we had a power law not for small s but for the tail. In order to investigate this we apply the test proposed in Ref. [12] to compare the performance of a lognormal tail versus a power-law tail. By tail we mean the part of the distribution that is above an arbitrary threshold value s_{cv} of the random variable; in other words, the tail is given by the domain $s > s_{cv}$. We expect s_{cv} to be relatively large. The test proceeds by computing the (residual) coefficient of variation cv of $\ln(s/s_{cv})$, which is

$$cv = \frac{1}{\sqrt{n_{cv} - 1}} \frac{\sqrt{\sum_i (\ln s_i - \overline{\ln s})^2}}{\overline{\ln s} - \ln s_{cv}}, \quad (3)$$

with $\overline{\ln s} = n_{cv}^{-1} \sum_i \ln s_i$, the sums comprising only the values s_i above s_{cv} (the “residual” values), and n_{cv} counting the number of data fulfilling this condition (in practice, s_{cv} is set equal to an empirical value, which is excluded then from the tail, due to the strict inequality $s > s_{cv}$).

It is a fundamental fact that this residual “logarithmic” coefficient of variation (3) is a decreasing function of the likelihood ratio between the truncated lognormal and the power law [37], so, a “large enough” likelihood ratio corresponds to a “small enough” cv and this is what allows one to replace the likelihood ratio by cv in the test (which has the clear advantage that one avoids the maximum-likelihood estimation of the parameters). Note also that the distribution of cv does not depend neither on the value of the exponent nor on the value of s_{cv} ; it only depends on n_{cv} .

As the power law can be considered a particular instance of a truncated lognormal (one with $\mu - \ln s_{cv} \rightarrow -\infty$ and $\sigma^2 \rightarrow \infty$, with μ and σ^2 the mean and variance of the associated untruncated normal distribution, which leads to power-law exponent $\beta = 1 + |\mu - \ln s_{cv}|/\sigma^2$, see Refs. [12, 37]), the likelihood ratio in this case will correspond to that of nested distributions, i.e., the power law is nested into the lognormal, which constitutes then a more general distribution than the former. So, it should be clear that a truncated lognormal will fit a tail at least as well as a power law. The point is if the improvement given by the lognormal is significant or not. Note that this test constitutes the uniformly most powerful unbiased test for power law against truncated lognormality [12, 37]. Considering different values of s_{cv} we will be able to determine if there is a transition between a power-law tail (cv close to 1) and a lognormal (cv far from 1) as the tail domain is increased; in other words, at which value

of s_{cv} a hypothetical power-law tail starts. We refer to such a value, if it exists (the value for which s_{cv} crosses the critical line given by the percentile corresponding to the desired confidence level) as s_{pl} . More details are given in Ref. [17].

Table I and Fig. 6 incorporate the results of this approach. For the critical values of the test we take the percentiles 5 and 95 of the distribution of cv , which leads to a 90 % confidence that the tail is power law, and a 95 % that the tail is power law in front of lognormal (cv cannot be larger than one for the lognormal, so the test has to be one-sided). We observe in the table that, except for the largest considered cell width ℓ , the cut-off value of the hypothetical power-law tail s_{pl} is in a range from 1500 to 10000 (inhabitants). The number of population clusters (cities) covered by that range (number of points in the tail, n_{pl}) turns out to be rather small, from 60 to 230, roughly.

We can use a variation of the logarithmic-coefficient-of-variation test (in fact, its original linear form, essentially) to rule out that the distribution of cluster size has an exponential tail, as was claimed in other contexts [38] (and already criticized in Refs. [39, 40]). If we compute the usual residual coefficient of variation of the cluster size (just dividing the standard deviation and the mean of the difference between s and a lower cut-off s'_{cv} , i.e., $s - s'_{cv}$) and compare with the results expected for an exponential variable [37], we get that cv turns out to be above the 0.95 percentile, which rules out the exponential tail for any value of s'_{cv} . Thus, the tail of the cluster-size distribution is not exponential. Similar conclusions are reached if one uses as a test statistic the mean of $s - s'_{cv}$ divided by its maximum [41].

Lognormal fits

As the existence of a power-law tail does not rule out the existence of a lognormal tail, and due to the low range of the power-law tail, and due also to the fact that we have ruled out the existence of a power law for small s , as a next step we explore the performance of a lognormal fit. Concretely, a lower-truncated lognormal (\ln) distribution is given by a probability density

$$f_{\ln}(s) = \sqrt{\frac{2}{\pi}} \left[\operatorname{erfc} \left(\frac{\ln s_{\ln} - \mu}{\sqrt{2}\sigma} \right) \right]^{-1} \frac{1}{\sigma s} \exp \left(-\frac{(\ln s - \mu)^2}{2\sigma^2} \right), \quad (4)$$

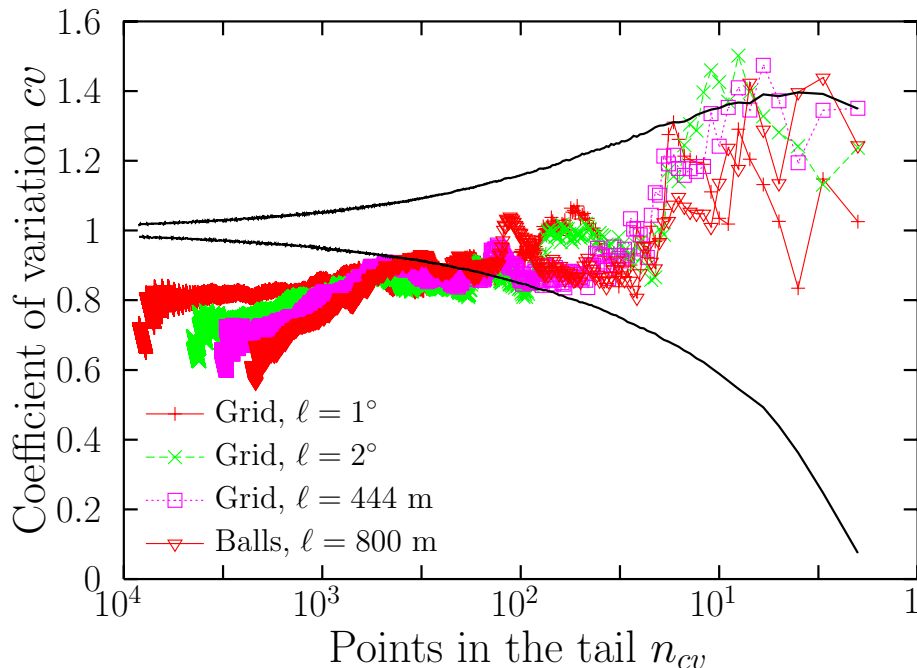


FIG. 6: Empirical value of the “residual logarithmic coefficient of variation” cv of the cluster population as a function of the number of residual points in the tail of the distribution, n_{cv} . Several examples are shown, corresponding to our three approaches. The solid lines correspond to the simulated 0.05 and 0.95 percentiles of the distribution of cv under the power-law null hypothesis. In all cases the first crossing below the 0.05 percentile takes place for n_{cv} around 100, which corresponds to n_{pl} in Table I. Note that the horizontal axis is reversed, to display the tail on the right side.

defined for s above the lower cut-off s_{ln} , with erfc the complementary error function, and μ and σ the mean and standard deviation of the associated untruncated normal distribution (e^μ turns out to be the scale parameter θ of $f_{ln}(s)$ and σ its shape parameter).

We fit this truncated lognormal distribution to our population data extending to log-normals the method introduced in Refs. [15, 42] for (continuous) power laws, consisting in maximum-likelihood estimation plus Kolmogorov-Smirnov goodness-of-fit test [17]. Although in recent years the recipe of Clauset et al. [5] has become very popular for power-law tails, we prefer the more intuitive approach of Refs. [15, 17, 42] (the reasons for our choice derive in part from the results of Refs. [14, 18] and also from the present research). The

extension of the method to lognormals has also been used in Ref. [17]. At the end, we arrive to optimal values of the three parameters s_{ln} , μ , and σ , which are included in Table I.

We see in the table how, in contrast to the power-law tail, the lognormal fit covers a considerable range of data, with a rather small value of s_{ln} (from 2 to 50 inhabitants, which leads to fits valid for more than 4 orders of magnitude in population) and a relatively large n_{ln} (either $n_{ln} \simeq N$ or $n_{ln} > 2000$). Inadequacy of the lognormal to fit the smallest values of s is expected due to the fact that the lognormal is a continuous distribution and s is a discrete variable.

The performance of the fits can be visually appreciated from Fig. 4; however, in order to stress the lognormal behavior, we apply a transformation which should lead to a linear plot in the lognormal case, see Fig. 7. This consists in representing

$$-\ln[\ln(e^\mu f_{ln}(e^\mu)) - \ln(sf(s))] \text{ versus } \ln \ln \frac{s}{e^\mu}$$

(restricted to $s > e^\mu$, to avoid the overlap with the branch $s < e^\mu$), or, equivalently, $[\ln(e^\mu f_{ln}(e^\mu)) - \ln(sf(s))]^{-1}$ versus $\ln s - \mu$ in additional logarithmic scale on each axis. Note that $f(s)$ refers to the empirical estimations of the density whereas $f_{ln}(e^\mu)$ refers to the theoretical distribution evaluated at $s = e^\mu$ (so, both μ and σ need to be estimated from data); note also that both axes are doubly logarithmic. Indeed, from Eq. (4) we get

$$-\ln \ln \left[\frac{e^\mu f_{ln}(e^\mu)}{sf(s)} \right] = -2 \ln \ln \frac{s}{e^\mu} + \ln(2\sigma^2),$$

which is a straight line with slope -2, in the variables defined above. We see in Fig. 7 how the straight behavior is more apparent than in the usual log-log plot of $f(s)$ versus s (Fig. 4), so we have an additional visual support for the lognormal fit in front of the power law. In fact, an additional shift by $2 \ln \ln \langle s \rangle$ is applied in the figure, in order to collapse the different distributions, which are merged into a single one.

Scaling to fix the lognormal parameters

From Table I one also realizes that the lognormal scale parameter e^μ increases with the grid or ball size ℓ but the shape parameter σ keeps constant, roughly (from 2.5 to 3, except for the largest ℓ). We now take advantage of the fact that the cluster-size distributions display scaling (at least approximately, see Fig. 5a). Therefore, for the different data sets

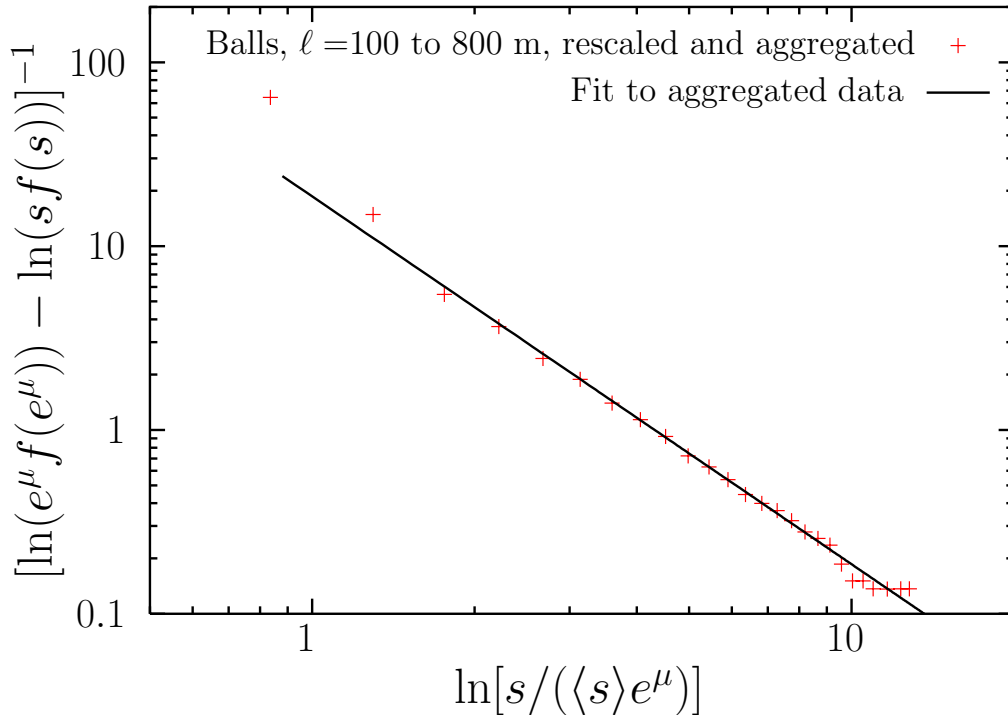


FIG. 7: Empirical probability density of rescaled cluster sizes ($s/\langle s \rangle$) aggregated for diverse values of ℓ (100, 200, 400, and 800 m), in the ball approach. The axes have been transformed to evaluate the goodness of the lognormal fit (Table I, continuous line). Plot equivalent to Fig 5(a), same data.

(corresponding to different ℓ) we can rescale s as $s/\langle s \rangle$ (as in Fig. 7), and then merge the different data sets into a single one, to which we can fit the lognormal distribution. The results in Table I confirm that a single lognormal can fit the rescaled distributions corresponding to different ℓ . Denoting the new value of the parameter μ as μ' (corresponding to the rescaled data), and taking into account the simple relation between the original and the rescaled data, we can express the value of μ of the original (not rescaled) distributions as $\mu = \mu' + \ln\langle s \rangle$, which shows indeed that μ increases with ℓ , as $\langle s \rangle$ increases with ℓ . Summarizing, and approximating the results from the table, we can write $e^\mu \simeq \langle s \rangle / e^{4.8}$ and $\sigma \simeq 3$. For the dependence of $\langle s \rangle$ on ℓ , using the data-collapse optimization method explained in Ref. [36], we find $\langle s \rangle \propto \ell^{0.8}$; nevertheless, the uncertainty of this exponent is rather large.

Power-law fits and comparison with lognormal

If one insists in fitting a power law to the tail of the distribution (taking advantage of the fact that the tail of a lognormal becomes asymptotically a power law, the tail being understood as the power-law tail defined by the logarithmic-coefficient-of-variation test as calculated above) we find exponents roughly close to but below $\beta = 2$ (the Zipf's value, see Table I); nevertheless, for the reasons mentioned above, we consider the power-law fit as anecdotic and prefer the lognormal fit, valid for a much larger range (Table I).

In fact, we can make a quantitative comparison between power-law and lognormal fits. For the power-law tail one already knows that the lognormal fit has to yield a likelihood at least as large as the one given by the power law (when both are fitted over the same range), but this difference is not significant (this is what the *cv*-test is about, allowing one to define the power-law tail in the range $s > s_{pl}$). In this sense, the power law always wins over the lognormal. However, we are interested in fitting not just a short power-law tail, but as much as possible of the bulk of the distribution (including the tail). So, on the one hand we have (model 1) the lognormal fit, in the range $s \geq s_{ln}$, and on the other hand (model 2) we have to consider the power-law tail complemented by the lognormal fit from s_{ln} to s_{pl} . Note that model 2 yields 4 parameters (μ and σ plus s_{pl} and β , considering s_{ln} as fixed); whereas model 1, the single lognormal, only has 2 parameters (μ and σ). In mathematical terms, the two models can be expressed as $f_1(s) = f_{ln}(s)$ for $s \geq s_{ln}$ and

$$f_2(s) = \begin{cases} f_{ln}(s) & \text{for } s_{ln} \leq s \leq s_{pl} \\ f_{pl}(s)n_{pl}/n_{ln} & \text{for } s > s_{pl}, \end{cases}$$

where the factor n_{pl}/n_{ln} ensures normalization (note that we do not impose continuity of $f_2(s)$ at $s = s_{pl}$, that would reduce the likelihood of the resulting fit).

We can compute the difference in log-likelihoods of both models as

$$\Delta \ln \hat{L} = \ln \hat{L}_2 - \ln \hat{L}_1 = \sum_{i=1}^{n_{ln}} (\ln f_2(s_i) - \ln f_1(s_i)),$$

(we only number the clusters with $s \geq s_{ln}$, and in increasing order, $s_1 \leq s_2 \leq \dots \leq s_{n_{ln}}$); however, as the two models coincide in the range $s_{ln} \leq s < s_{pl}$, the comparison of likelihoods only needs to be done at the tail, $s \geq s_{pl}$, and thus,

$$\Delta \ln \hat{L} = \sum_{i=n_{ln}-n_{pl}+1}^{n_{ln}} (\ln f_{pl}(s_i; \beta, s_{pl}) - \ln f_{ln}(s_i; \mu, \sigma, s_{pl})),$$

where we have made explicit the dependence on the parameters. Note that for the lognormal we have replaced its lower cut-off s_{ln} by s_{pl} , this is what allows to eliminate the factor n_{pl}/n_{ln} that multiplied $f_{pl}(s)$ as in this way both distributions are normalized in the range $s \geq s_{pl}$.

As expected, this difference of log-likelihoods turns out to be negative (see Table II), which means that model 1 (single lognormal) would be favored; however, this comparison does not take into account the different number of parameters. If we introduce the Akaike information criterion, $AIC = 2k - 2 \ln \hat{L}$, where k is the number of parameters, we get $\Delta AIC = 4 - 2\Delta \ln \hat{L}$, which is positive, favoring more clearly the lognormal model (Table II again). The Bayesian information criterion, $BIC = k \ln n_{ln} - 2 \ln \hat{L}$ leads to $\Delta BIC = 2 \ln n_{ln} - 2\Delta \ln \hat{L}$, with the same conclusion. In any case, the lognormal fit is preferred.

Note that when only the tail is compared, the power law has one parameter whereas the lognormal has two, which favors the former; however, considering the whole range $s \geq s_{ln}$, the situation is reversed, as the power-law tail combined with the lognormal bulk has four parameters, which favors the single lognormal, despite the fact that the difference in log-likelihood does not change. Note also that the difference in AIC does not depend on the number of data in the fit, whereas ΔBIC does; in fact, the more data, the better the simple (lognormal) fit.

Finally, in order to allow some comparison, we apply the same test as in Ref. [11], which is Pearson's chi-squared test. We consider just two classes, $s_{ln} \leq s < s_{pl}$ and $s \geq s_{pl}$, and compute $x^2 = \sum_{k=1}^2 (E_k - O_k)^2 / E_k$, where O_k is the observed number of clusters in the k -th class (either $n_{ln} - n_{pl}$ or n_{pl}) and E_k is the expected number of clusters from the lognormal fit, which is either $(1 - q_{tail})n_{ln}$ or $q_{tail}n_{ln}$, with q_{tail} the probability that the lognormal fit assigns to the tail. This is calculated as

$$q_{tail} = \operatorname{erfc} \left(\frac{\ln s_{pl} - \mu}{\sqrt{2}\sigma} \right) / \operatorname{erfc} \left(\frac{\ln s_{ln} - \mu}{\sqrt{2}\sigma} \right).$$

The results, included in Table II show that the values of x^2 are in all cases too small to reject the lognormal fit.

Dragon-king effect

It is remarkable that, although the cluster associated to the city of Barcelona could be considered to have the status of dragon king (in the Sornette's sense of a very large outlier in s [43]), with a population much larger than that of the second largest cluster (at least a 5-fold larger, depending on ℓ), with a clear deviation therefore with respect Zipf's law in terms of the rank-size representation, this does not cause the rejection neither of the lognormal fit nor of the power-law tail for the cluster-size distribution. In other words, in terms of the distribution of sizes, the fits are not affected by the dragon-king effect.

We can go one step further and study the influence of the largest cluster on the distribution, just removing it. The results, show a very similar behavior, except that the value of the exponent β gets somewhat larger. We conclude that, from the point of view of the distribution of cluster sizes, and for the present study, the largest cluster (which could be considered a dragon king) does not change the character of the tail, and only modifies a little the value of the parameters.

Origin of the large variability in city sizes

Our approach allows us to investigate the origin of the broadness of the distribution of the size of population clusters (i.e., the size of cities, in our definition). In the grid approach, the distribution $f(s)$ arises from the sum of the number of inhabitants h of each cell (with a distribution given by $f(h)$) along each cluster, so, $f(s)$ depends both on $f(h)$ and on the distribution of the number of cells per cluster; nevertheless, this is not enough, as one needs to take into account that the values of h are not independent from cell to cell, i.e., there are spatial correlations in the values of h (highly populated cells tend to be surrounded by highly populated cells, and reciprocally). This is in fact an obvious fact, but we can demonstrate the relevance of correlations in the values of h eliminating these correlations and looking for the resulting $f(s)$.

We eliminate the correlations just reshuffling the values of h among occupied clusters; this keeps the distribution $f(h)$ and the spatial extend of clusters unchanged. The results are displayed in Fig. 8, showing that the resulting randomized $f(s)$ is less broad than the original $f(s)$; in particular, no sign of an approximate power-law tail with exponent close to

2 is found, leading to the conclusion that the main cause of the large variability in city size (and the cause of the rough Zipf-like behavior) are spatial correlations. This means that the (fractal) shape of cities is not enough to explain their population distribution. Above we mentioned the advantages of the ball approach over the grid approach; however, notice that this reshuffling procedure can only be performed under the grid approach, so, both approaches can be considered as complementary.

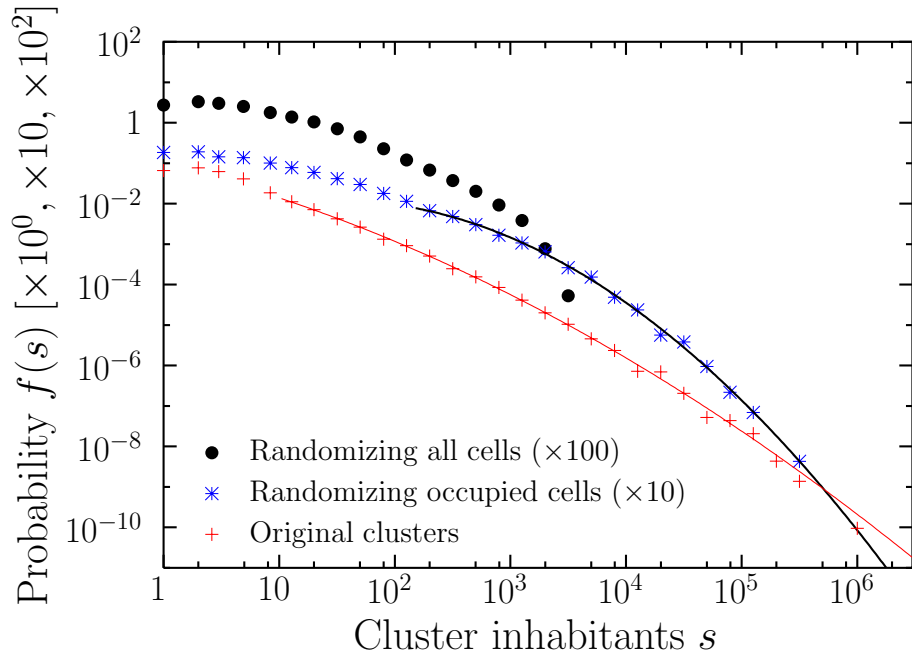


FIG. 8: Comparison of the original distribution of cluster sizes $f(s)$ with the distribution of cluster sizes obtained when the values h of the population of each cell are randomized between occupied cells. The less interesting case in which the values of h are randomized between all cells (occupied and unoccupied) is also shown. The example shown corresponds to the grid-in-km approach, with $\ell = 222$ m.

CONCLUSIONS

Population data of high spatial resolution allows one to locate individuals and to build clusters of them in space. If the locations of individuals correspond to their residence place (as it is in our study), these clusters constitute a natural definition of human settlements or, broadly speaking, cities. We have scrutinized the distribution of the number of individ-

uals in the clusters obtained in this way (natural-city size) with up-to-date data-analysis tools. On the one hand, scaling analysis allows us to rule out the existence of a power-law size distribution with exponent $\alpha > 1$ for the smallest cities; on the other hand, the logarithmic-coefficient-of-variation test shows that a power-law tail has a very limited range of applicability. Instead, a lognormal fit holds for a considerable part of the data and does not only yield a higher likelihood than a model joining a lognormal part in the bulk plus a power-law tail, but also has less parameters, which makes the lognormal to be clearly supported by model comparison using AIC or BIC.

Obviously, we do not dispute that the US population distribution, as measured from its census, is better described by a power law than by a lognormal at its tail, as claimed in other studies [11, 12]. But it could be that the bad performance of the lognormal at the tail of the US city distributions is due to the fact that it is a pure (untruncated) lognormal which is fitted, and not a truncated one, as used here. In any case, our example sets clearly that other datasets and/or other definition of cities can lead to a better characterization by (truncated) lognormal distributions. This implies that universality [44] does not seem to be a characteristic of city-size distributions, as also found for other complex systems, for instance, wildfires [17, 45].

Our spatial-grid based approach also allows us to stress the importance of spatial correlations in the broadness of the city-size distribution; in other words, knowledge of the area occupied by cities together with the distribution of individuals in small grids does not allow to explain the number of inhabitants in cities. Finally, we have seen how, although our largest cluster (associated to the city of Barcelona) has the status of a dragon-king, it does not have an important influence on the city-size distribution. The reason is that, under the distribution-of-sizes representation (in contrast to the rank-size approach), the largest cluster counts just as one single realization of the random variable (in contrast to more than one million counts of individuals from that cluster in the other approach), and thus, it has a very small statistical weight.

On a further step, one could fit to the data a power law truncated also from above (a power law defined in a range $s_{pl1} \leq s \leq s_{pl2}$, where these parameters are optimized by the fitting [15, 17]). This leads to exponents α in the range 1.6 to 1.8, valid for several orders of magnitude, between 3 and 4, starting at values of s around 500 or higher. In some cases, the upper truncation point turns out to be above s_{max} (the largest cluster), which means

that the fitting method is not able to distinguish the power-law tail (which has a somewhat different power-law exponent β). In any case, the lognormal fit turns out to be valid in a wider range, and it is thus preferred. In a future work one could compare the performance of the lognormal with that of a double power law [17], which has been proposed for other Zipf-like systems [46, 47].

ACKNOWLEDGEMENTS

We are indebted to E. Suñé from IDESCAT, S. Manrubia, J. del Castillo, and I. Serra. A. C. has participated in the grant from the Spanish MINECO awarded to the Barcelona Graduate School of Mathematics (BGSMath) under the María de Maeztu Program (grant MDM-2014-0445), as well as in the projects FIS2012-31324, FIS2015-71851-P (MINECO), and FIS-PGC2018-099629-B-I00 (MICIU) and in 2014SGR-1307 (AGAUR). F.U. and E.A. acknowledge the funding of PGC2018-101643-B-I00 (MICIU) and the EPSRC grant EP/M023583/1, respectively.

-
- [1] M. Barthelemy. The statistical physics of cities. *Nature Rev. Phys.*, 1(6):406–415, 2019.
 - [2] L. Bettencourt and G. West. A unified theory of urban living. *Nature*, 467:912–913, 2010.
 - [3] G. K. Zipf. *Human Behavior and the Principle of Least Effort*. Addison-Wesley, 1949.
 - [4] R. L. Axtell. Zipf distribution of U.S. firm sizes. *Science*, 293:1818–1820, 2001.
 - [5] A. Clauset, C. R. Shalizi, and M. E. J. Newman. Power-law distributions in empirical data. *SIAM Rev.*, 51:661–703, 2009.
 - [6] S. Pueyo and R. Jovani. Comment on “A keystone mutualism drives pattern in a power function”. *Science*, 313:1739c–1740c, 2006.
 - [7] L. A. Adamic and B. A. Huberman. Zipf’s law and the Internet. *Glottom.*, 3:143–150, 2002.
 - [8] I. Moreno-Sánchez, F. Font-Clos, and A. Corral. Large-scale analysis of Zipf’s law in English texts. *PLoS ONE*, 11(1):e0147073, 2016.
 - [9] J. Serrà, A. Corral, M. Boguñá, M. Haro, and J. Ll. Arcos. Measuring the evolution of contemporary western popular music. *Sci. Rep.*, 2:521, 2012.
 - [10] J. Eeckhout. Gibrat’s law for (all) cities. *Amer. Econ. Rev.*, 94(5):1429–1451, 2004.

- [11] M. Levy. Gibrat’s law for (all) cities: Comment. *Amer. Econ. Rev.*, 99(4):1672–1675, 2009.
- [12] Y. Malevergne, V. Pisarenko, and D. Sornette. Testing the Pareto against the lognormal distributions with the uniformly most powerful unbiased test applied to the distribution of cities. *Phys. Rev. E*, 83:036111, 2011.
- [13] E. P. White, B. J. Enquist, and J. L. Green. On estimating the exponent of power-law frequency distributions. *Ecol.*, 89:905–912, 2008.
- [14] A. Corral, F. Font, and J. Camacho. Non-characteristic half-lives in radioactive decay. *Phys. Rev. E*, 83:066103, 2011.
- [15] A. Deluca and A. Corral. Fitting and goodness-of-fit test of non-truncated and truncated power-law distributions. *Acta Geophys.*, 61:1351–1394, 2013.
- [16] A.-L. Barabási. Love is all you need. Clauset’s fruitless search for scale-free networks. *unpublished*, 2018.
- [17] A. Corral and A. González. Power law distributions in geoscience revisited. *Earth Space Sci.*, 6(5):673–697, 2019.
- [18] I. Voitalov, P. van der Hoorn, R. van der Hofstad, and D. Krioukov. Scale-free Networks Well Done. *arXiv*, 1811.02071, 2018.
- [19] E. Arcaute, E. Hatna, P. Ferguson, H. Youn, A. Johansson, and M. Batty. Constructing cities, deconstructing scaling laws. *J. Roy. Soc. Interf.*, 12(102), 2015.
- [20] J. C. Leitão, J. M. Miotto, M. Gerlach, and E. G. Altmann. Is this scaling nonlinear? *Open Sci.*
- [21] R. Peng. The reproducibility crisis in science: A statistical counterattack. *Significance*, 12(3):30–32, 2015.
- [22] R. L. Wasserstein and N. A. Lazar. The ASA’s statement on p-values: Context, process, and purpose. *Am. Stat.*, 70(2):129–133, 2016.
- [23] H. D. Rozenfeld, D. Rybski, J. S. Andrade, M. Batty, H. E. Stanley, and H. A. Makse. Laws of population growth. *Proc. Natl. Acad. Sci. USA*, 105(48):18702–18707, 2008.
- [24] B. Jiang and T. Jia. Zipf’s law for all the natural cities in the United States: a geospatial perspective. *Int. J. Geograp. Inform. Sci.*, 25(8):1260–1281, 2011.
- [25] B. Jiang, J. Yin, and Q. Liu. Zipf’s law for all the natural cities around the world. *arxiv.org*, 1402.2965, 2014.
- [26] E. Arcaute, C. Molinero, E. Hatna, R. Murcio, C. Vargas-Ruiz, A. P. Masucci, and M. Batty.

- Cities and regions in Britain through hierarchical percolation. *Roy. Soc. Op. Sci.*, 3(4), 2016.
- [27] E. S. Luis. Hacia un registro estadístico de territorio. *XXXV Congreso Nacional de Estadística e Investigación Operativa, IX Jornadas de Estadística Pública*, 2015 (in Spanish).
- [28] C. D. V. Orozco, J. Golay, and M. Kanevski. Multifractal portrayal of the Swiss population. *arXiv*, 1308.4038, 2013.
- [29] F. Sémécurbe, C. Tannier, and S. G. Roux. Spatial distribution of human population in France: Exploring the modifiable areal unit problem using multifractal analysis. *Geograp. Anal.*, 48(3):292–313, 2016.
- [30] D. Stauffer and A. Aharony. *Introduction To Percolation Theory*. CRC Press, 2nd edition, 1994.
- [31] K. Christensen and N. R. Moloney. *Complexity and Criticality*. Imperial College Press, London, 2005.
- [32] E. Simoudis, J. Han, and U. M. Fayyad, editors. *Proceedings of the Second International Conference on Knowledge Discovery and Data Mining (KDD-96), Portland, Oregon, USA*. AAAI Press, 1996.
- [33] M. Cristelli, M. Batty, and L. Pietronero. There is more than a power law in Zipf. *Sci. Rep.*, 2:812, 2012.
- [34] A. Corral, I. Serra, and R. Ferrer-i-Cancho. The distinct flavors of Zipf’s law in the rank-size and in the size-distribution representations, and its maximum-likelihood fitting. *arXiv*, 1908:01398, 2019.
- [35] A. Corral. Scaling in the timing of extreme events. *Chaos. Solit. Fract.*, 74:99–112, 2015.
- [36] A. Deluca and A. Corral. Scale invariant events and dry spells for medium-resolution local rain data. *Nonlinear Proc. Geophys.*, 21:555–567, 2014.
- [37] J. del Castillo and P. Puig. The best test of exponentiality against singly truncated normal alternatives. *J. Am. Stat. Assoc.*, 94:529–532, 1999.
- [38] S. Bernhardsson, L. E. Correa da Rocha, and P. Minnhagen. The meta book and size-dependent properties of written language. *New J. Phys.*, 11:123015, 2009.
- [39] F. Font-Clos, G. Boleda, and A. Corral. A scaling law beyond Zipf’s law and its relation to Heaps’ law. *New J. Phys.*, 15:093033, 2013.
- [40] A. Corral and F. Font-Clos. Dependence of exponents on text length versus finite-size scaling for word-frequency distributions. *Phys. Rev. E*, 96:022318, 2017.

- [41] P. Rochet and I. Serra. The mean/max statistic in extreme value analysis. *arXiv*, 1606.08974, 2016.
- [42] O. Peters, A. Deluca, A. Corral, J. D. Neelin, and C. E. Holloway. Universality of rain event size distributions. *J. Stat. Mech.*, P11030, 2010.
- [43] D. Sornette. Dragon-kings, black swans and the prediction of crises. *Int. J. Terraspace Sci. Eng.*, 2(1):1–18, 2009.
- [44] H. E. Stanley. Scaling, universality, and renormalization: Three pillars of modern critical phenomena. *Rev. Mod. Phys.*, 71:S358–S366, 1999.
- [45] S. Hantson, S. Pueyo, and E. Chuvieco. Global fire size distribution: from power law to log-normal. *Int. J. Wildl. Fire*, 25:403–412, 2016.
- [46] R. Ferrer i Cancho and R. V. Solé. Two regimes in the frequency of words and the origin of complex lexicons: Zipf’s law revisited. *J. Quant. Linguist.*, 8(3):165–173, 2001.
- [47] M. Gerlach and E. G. Altmann. Stochastic model for the vocabulary growth in natural languages. *Phys. Rev. X*, 3:021006, 2013.

TABLE I: Population-cluster properties obtained from the grid-in-degrees, grid-in-km, and the ball approaches (N and s_{max}); results from the logarithmic-coefficient-of-variation test (s_{pl} and n_{pl}), together with a power-law fit (β); and results from the lognormal fit. N is total number of clusters, s_{max} is the size of the largest one (always associated to Barcelona), s_{pl} is the cut-off value for the power-law tail, n_{pl} is the number of clusters in that tail, s_{ln} and n_{ln} are the equivalent for the lognormal fit, r is the number of orders of magnitude of that fit ($r = \log_{10}(s_{max}/s_{ln})$), μ and σ are the selected lognormal parameters, and p is the p -value of the lognormal fit. The last row for each approach corresponds to the aggregation for different ℓ of the rescaled variable $s/\langle s \rangle$. The results for municipalities are also included, using data from IDESCAT at January 1, 2016. The values of s_{ln} swept are 50 per order of magnitude and the p -value is computed from 1000 Monte-Carlo simulations.

ℓ	N	s_{max}	s_{pl}	n_{pl}	β	s_{ln}	r	n_{ln}	μ	σ	p
1°	8376	$1.98 \cdot 10^6$	6893	134	1.95	52.5	4.576	2450	2.120	3.102	0.21
2°	4465	$2.48 \cdot 10^6$	10216	91	1.95	13.2	5.275	2571	3.138	2.975	0.23
4°	2976	$3.05 \cdot 10^6$	13033	57	1.83	8.3	5.565	2082	3.643	2.869	0.40
8°	1827	$4.06 \cdot 10^6$	1473	203	1.72	5.2	5.888	1470	3.933	2.814	0.25
16°	694	$6.00 \cdot 10^6$	1462	101	1.69	2.1	6.458	635	4.665	2.653	0.33
32°	102	$7.27 \cdot 10^6$	236	61	1.47	14.5	5.702	82	6.426	2.415	0.25
1 to 8°	17644	$2.18 \cdot 10^3$	-	-	-	0.02	5.059	7998	-4.735	3.064	0.44
111 m	10258	$1.94 \cdot 10^6$	7468	125	1.96	50.1	4.587	2810	1.542	3.176	0.23
222 m	4966	$2.11 \cdot 10^6$	9763	92	1.90	10.5	5.304	2972	2.772	3.062	0.26
444 m	3209	$3.05 \cdot 10^6$	6913	98	1.82	12.0	5.404	2047	3.604	2.866	0.21
889 m	2095	$3.62 \cdot 10^6$	1462	228	1.72	6.3	5.758	1613	3.980	2.788	0.32
1778 m	922	$6.00 \cdot 10^6$	1462	123	1.71	3.0	6.298	814	4.532	2.615	0.32
3556 m	159	$7.18 \cdot 10^6$	635	70	1.59	22.9	5.496	126	6.598	2.131	0.27
111 to 889	20528	$2.62 \cdot 10^3$	-	-	-	0.03	4.998	8458	-4.843	3.076	0.27
100 m	10263	$1.88 \cdot 10^6$	6731	135	1.95	26.3	4.853	3875	0.957	3.305	0.28
200 m	5029	$2.41 \cdot 10^6$	9764	95	1.95	14.5	5.222	2833	3.131	2.921	0.32
400 m	3363	$2.66 \cdot 10^6$	11263	74	1.86	7.6	5.545	2358	3.466	2.937	0.23
800 m	2262	$3.38 \cdot 10^6$	2736	163	1.74	6.3	5.729	1744	3.997	2.782	0.39
1600 m	1059	$5.08 \cdot 10^6$	1492	148	1.71	3.0	6.226	941	4.578	2.640	0.30
3200 m	220	$7.14 \cdot 10^6$	486	93	1.61	251.	4.454	129	3.959	2.824	0.27
100 to 800	20916	$2.54 \cdot 10^3$	-	-	-	0.02	5.085	9622	-4.749	3.051	0.21

TABLE II: Model comparison between single lognormal fit (model 1, with 2 parameters) and lognormal bulk plus power-law tail (model 2, with 4 parameters). Differences are computed as model 2 minus model 1. The outcome always favors the simpler model 1, lognormal. Results for the chi-squared test explained in the text (see also [11]) applied to model 1 are also included and confirm that the lognormal fit cannot be rejected.

ℓ	$\Delta\hat{L}$	ΔAIC	ΔBIC	χ^2 model 1
1°	-1.269	6.538	12.334	0.0012
2°	-1.105	6.209	11.231	0.0009
4°	-0.632	5.264	9.350	0.4684
8°	-1.381	6.761	13.388	0.8624
16°	-1.603	7.207	12.437	0.9272
32°	-0.610	5.220	9.441	0.8631
111 m	-1.152	6.305	11.961	0.0006
222 m	-1.380	6.760	11.804	0.2616
444 m	-1.158	6.316	11.486	0.6692
889 m	-1.446	6.893	13.752	1.2255
1778 m	-2.179	8.358	13.982	0.6197
3556 m	-1.221	6.441	10.938	0.0000
100 m	-1.030	6.060	11.870	0.1532
200 m	-1.413	6.826	11.934	0.0147
400 m	-1.346	6.692	11.300	0.2874
800 m	-1.364	6.728	12.916	1.3501
1600 m	-1.492	6.983	12.978	0.5327
3200 m	-1.658	7.317	12.382	0.3306
municip.	-1.559	7.118	12.519	0.0054